Design and In-Situ Characterization of Catalyst Surfaces

Department of Materials Molecular Science
Division of Electronic Structure

TADA, Mizuki
Associate Professor (–March, 2013)*

MURATSUGU, Satoshi
Assistant Professor†

MAITY, Niladri	Post-Doctoral Fellow
ZHANG, Shenghong	Post-Doctoral Fellow
SAIDA, Takahiro	Post-Doctoral Fellow
WAKI, Minoru	Post-Doctoral Fellow
SODE, Aya	Post-Doctoral Fellow
KITYAKARN, Sutasinee	Post-Doctoral Fellow
TRAN, Quang Thuong	JENESYS Program Visiting Scientist
WANG, Fei	Graduate Student
ISHIGURO, Nozomu	Graduate Student‡
USUI, Chika	Technical Fellow
GONDO, Makiko	Technical Fellow
FUKUTOMI, Yukiyo	Secretary

We have focused on the preparation of new catalyst surfaces by using metal complexes, metal nanoparticles, and metal oxides and in situ characterization of solid catalysts under catalyst working conditions.

1. Preparation and Discontinuous Property of Methane Steam Reforming of Ni/Ordered $Ce_2Zr_2O_x$ Catalysts¹⁾

Methane steam reforming is one of the key reactions to produce hydrogen. We prepared Ni catalysts on an ordered $Ce_2Zr_2O_x$ solid-solution support (x = 7–8) with a regular arrangement of Ce and Zr ions for CH_4 steam reforming to produce H_2 and CO. The catalytic performance of the Ni/$Ce_2Zr_2O_x$ catalysts strongly depended on the oxygen content of $Ce_2Zr_2O_x$, and we found a unique discontinuity in the CH_4 steam-reforming activity at x = 7.5 (Figure 1).

Ni/$Ce_2Zr_2O_7$ catalyst was stable, resulting in a remarkably catalytic performance. The discontinuity in the catalytic performance at x = 7.5 may be related to the oxygen storage capacity of $Ce_2Zr_2O_x$. The reduction of NiO_y strongly depended on the nature of the $Ce_2Zr_2O_x$ support. In the range of $7 \le x < 7.5$, Ni and $Ce_2Zr_2O_x$ were reduced to the metallic state and the $Ce_2Zr_2O_7$ phase, respectively, under the reaction conditions; the reduction was due to CH_4. In the range of $7.5 \le x \le 8$, however, NiO_y was converted to NiO and $Ce_2Zr_2O_x$ remained unchanged under the reaction conditions. The oxidation of Ni nanoparticles on $Ce_2Zr_2O_x$ ($7.5 \le x \le 8$) was due to H_2O.

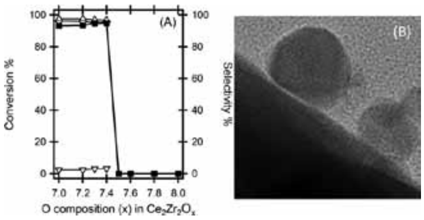

Figure 1. (A) CH_4 steam-reforming performance of Ni/$Ce_2Zr_2O_x$ at 973 K. The oxygen content x was changed by the reaction with O_2 and Ni/$Ce_2Zr_2O_7$ at 773 K ■ (with bold line): CH_4 conv.%, △: CO selectivity %, ▽: CO_2 selectivity %, and ◇: H_2 selectivity %. (B) A TEM image of the Ni catalyst.

The oxygen storage and release processes rapidly occur at $x < 7.5$ compared with $x \ge 7.5$. In the range of $7 \le x < 7.5$, lattice oxygen atoms in $Ce_2Zr_2O_x$ readily migrate from the bulk to the surface, at which they react with CH_4 to form the resultant $Ce_2Zr_2O_7$ phase. The transport of oxygen atoms at the interface between NiO_y nanoparticles and a $Ce_2Zr_2O_x$ support and/or the spillover of oxygen atoms at the boundary may be key issues in the chemical event.

2. Imaging of Pt/C Cathode Catalyst Layers in MEA for PEFC by X-Ray Laminography XAFS²⁾

Polymer electrolyte fuel cells (PEFCs) are among the most efficient clean energy technologies, but practical application in automobiles remains challenging because of the high cost and insufficient durability of cathode catalysts. The deactivation and unfavorable dissolution of Pt catalysts at cathode under PEFC operating conditions are serious to be tackled. However, direct observation of the chemical states of Pt catalysts in a membrane electrode assembly (MEA) for PEFC is not achieved in a non-destructive manner.

X-ray Computed Laminography (XCL) is applicable to partial three-dimensional imaging of such a shaped sample. In XCL, the rotation axis of a sample is not fixed at 90° with respect to incident X-ray beam, and the sample is inclined. We succeeded in measuring XCL-XAFS combining XCL imaging technique and XAFS spectroscopy by changing the energies of incident X-rays for XCL. The reconstruction images of XCL-XAFS revealed not only the morphology of cathode catalyst layer but also the distribution of Pt catalysts inside the catalyst layer.

The spatio-distribution of the Pt catalysts was visualized by mapping Pt L_{III}-edge intensity, which corresponds to a difference in the intensity of X-ray absorption at 11.572 keV (isosbestic point of Pt and PtO_2) from that at 11.496 keV (before Pt L_{III}-edge). We reconstructed 3D images of the distributions of Pt nanoparticles in the cathode catalyst layer in the fresh and degraded MEAs. The distribution of the Pt catalyst remarkably changed after the degradation process of MEA, and several aggregation spots of the Pt catalyst and large cavities in the cathode catalyst layer were observed (Figure 2 (A)). The Pt distribution was heterogeneous throughout the entire cathode catalyst layer, which suggests that Pt migration, aggregation, and cracking spread throughout the cathode catalyst layer in the degraded MEA.

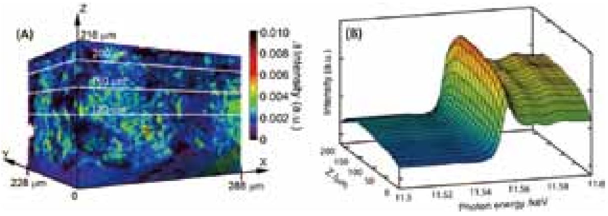

Figure 2. (A) The distribution of the Pt catalyst inside the cathode catalyst layer of the degraded MEA by XCL-XAFS. (B) Depth-resolved XCL-XANES spectra for the degraded MEA.

Depth-resolved XANES spectra were successfully obtained by integrating 3D-Laminography-XANES spectra over the X–Y plane at each depth in the X-ray energy range of 11.439–11.608 keV (Figure 2 (B)). Difference in the edge intensity of the Pt L_{III}-edge XANES spectra indicates difference in the Pt quantity in the MEAs along the Z depth. A series of depth-resolved Laminography-XANES spectra of the degraded MEA were wavy to the Z depth, probably reflecting the degradation of the MEA.

The newly developed XCL-XAFS technique provided the three-dimensional images of Pt quantity in the fresh and degraded MEAs enabled the visualization of aggregation behavior induced under PEFC operating processes. The 3D-Laminography-XAFS method would be promising for visualizing heterogeneous structural information in MEAs in order to address critical issues on the performance and property of practical PEFCs.

3. Ethynylpyridine-Functionalized Pt/Al_2O_3 Catalyst with Induced Chirality for Hexose Sugar Oxidation[3]

Uronic acids are monosaccharide derivatives in which primary hydroxyl group at the terminal carbon is oxidized to a carboxylic acid. To prepare glucuronic acid, the hydroxyl group at the 6-position of glucose must be selectively oxidized without over-oxidizing the secondary alcohols at other positions. We prepared a heterogeneous Pt nanoparticle catalyst with a sugar-binding ethynylpyridine (EPy) site (EPy/Pt/Al_2O_3) for the selective oxidation of hexose sugars to their corresponding uronic acids. Compared with a non-EPy-functionalized Pt/Al_2O_3 catalyst, EPy/Pt/Al_2O_3 enhanced reaction rates for the selective oxidation of the 6-OH groups of hexose sugars.

Titration with octyl β-D-glucopyranoside monitored by UV/vis and CD spectroscopy revealed that EPy acted as a binding site for hexose sugar, resulting in a complex of the EPy moiety and the hexose sugar with induced chirality. When Oct-β-D-Glc was added, an induced CD (ICD) signal with negative Cotton effect was observed in the region of the EPy ligand absorption (Figure 3 (A)). An ICD signal with positive Cotton effect was also observed after the addition of the enantiomer, octyl β-L-glucopyranoside. The ICD signals of the EPy ligand on the EPy/Pt/Al_2O_3 catalyst surface depended on the chirality of the hexose sugars, which demonstrated that binding interaction between the EPy ligand and the hexose sugars existed on the catalyst surface (Figure 3 (B)). The positive binding of the hexose sugars to EPy through intermolecular host–guest interaction would be enhanced the reaction rates of the selective oxidation on the Pt nanoparticle catalyst.

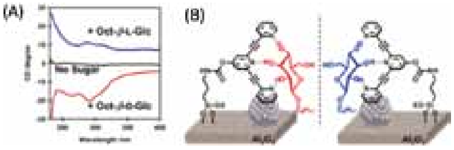

Figure 3. (A) CD spectra of the mixture of Pt/Al_2O_3 and octyl β-glucopyranoside in CH_2Cl_2. (B) The suggested host–guest interaction of EPy and the hexose sugar.

References

1) M. Tada, S. Zhang, S. Malwadkar, N. Ishiguro, J. Soga, Y. Nagai, K. Tezuka, H. Imoto, S. O. –Y. –Matsuo, S. Ohkoshi and Y. Iwasawa, *Angew. Chem., Int. Ed.* **51**. 9361–9365 (2012) (Hot Paper).

2) T. Saida, O. Sekizawa, N. Ishiguro, K. Uesugi, M. Hoshina, T. Uruga, S. Ohkoshi, T. Yokoyama and M. Tada, *Angew. Chem., Int. Ed.* **51**. 10311–10314 (2012).

3) M. Waki, S. Muratsugu and M. Tada, *Chem. Commun.* **49**. 7283–7285 (2013) (Inside Back Cover).

Award

KITYAKARN, Sutasinee; Poster Prize Award (ISHHC-16).

---

* Present Position; Professor, Research Center for Materials Science, Nagoya University

† Present Address; Graduate School of Science, Nagoya University

‡ carrying out graduate research on Cooperative Education Program of IMS with The University of Tokyo